THE JOURNAL OF Ammonia Energy

Available online at

jae.cardiffuniversitypress.org

ISSN **2752-7735**
The Journal of Ammonia Energy 01 (2023) 021–032

Cardiff University Press | Gwasg Prifysgol Caerdydd

Combustion Characteristics of a Novel Ammonia Combustor Equipped with Stratified Injection for Low Emission

Mashruk S[a*], Alnasif A[a,b], Yu C[c], Thatcher J[d], Rudman J[e], Peronski L[f], Chiong M-C[g], Valera-Medina A[a]

[a]*College of Physical Sciences and Engineering, Cardiff University, Queen's Building, Cardiff CF24 3AA, United Kingdom.*
[b]*Engineering Technical College of Al-Najaf, Al-Furat Al-Awsat Technical University, Najaf, 31001, Iraq.*
[c]*Institute of technical Thermodynamics, Karlsruhe Institute of Technology (KIT), Karlsruhe, Germany.*
[d]*Element Energy, Exchequer Court, 33 St Mary Axe, London EC3A 8AA, United Kingdom.*
[e]*Flogas Britain Limited, Fourth Way, Avonmouth, Bristol BS11 8DL, United Kingdom.*
[f]*Enertek International, 1 Malmo Road, Sutton Fields, Kingston Upon Hull, HU7 0YF, United Kingdom.*
[g]*Department of Mechanical Engineering, Faculty of Engineering, Technology & Built Environment, UCSI University, 56000 Kuala Lampur, Malaysia.*

Abstract

Ammonia – a carbon free fuel- is being considered by various research groups and organizations as a potential alternative fuel to tackle some global warming issues of the 21st century. However, ammonia faces some challenges as a fuel, particularly, the production of unwanted NOx and unburned ammonia traces at the back end of combustion systems accompanied by unstable flame regimes. Therefore, new concepts are currently being developed to address these challenges whilst also providing stable, high-power operation. This work presents a newly designed stratified combustion system for gas turbines capable of operating with both premixed and stratified modes. The system has been initially evaluated using these two modes employing solely hydrogen and ammonia. Increase of hydrogen stratification resulted in the reduction of NO and NO_2, while N_2O slightly increased due to the reduction of fuel in the premixed system. Further tests were conducted to evaluate the potential of the systems to replace fossil fuels. Previous work done using methane as the fuel-to-be-replaced has shown interesting trends in terms of emissions and stability. Thus, to progress on the subject, the work conducted here attempted propane/ammonia/hydrogen using this innovative strategy. Results denoted how stratification has a strong impact on NOx production at the flame front, whilst the mechanism of flame stabilization of the new burner enables large operability regions under a great variety of fuel combinations. Strategic injection setups were identified, whilst the best propane/ammonia/hydrogen blends for stability and emissions reduction are also detailed for further implementation in larger systems.

Received: 12th Dec 22; Accepted: 11th May 23; Published: 4th July 23

Keywords: ammonia combustion, stratified injection, propane replacement, stability, NOx emissions reduction.

Introduction

Ammonia appears as a chemical with the potential of replacing fossil fuels in the power sector. The net zero carbon features of ammonia with its specific storage characteristics make it a good replacement of various fossil fuels. Although it is known that the use of ammonia compared to fossils brings down the power outputs of power systems (with a Low Heating Values of 18.61 MJ/kg compared to 46.34 MJ/kg in propane), the chemical is still one of the most energy dense fuels in the variety of net zero options commercially available, hence opening the opportunity for the development of more efficient systems that can bridge the energy gap between fossil and zero carbon alternatives. For these reasons, novel research has been conducted on the efficient use of ammonia blends in combustion systems, trying to tackle some of the most challenging aspects of this fuel, ie. NOx emissions and flame stability.

Ammonia studies go back to fundamental flames that were analyzed to determine the propagation and flame speed when replacing fossil fuels by ammonia [1]. Those studies denoted the low flame speed of ammonia compared to other fuels, hence making challenging its implementation in industrial applications. The works expanded to gas turbines that at the time showed low efficiencies, leading to the end of those initiatives to use the molecule in the power sector [1]. However, the new restrictions in power production due to climate change have

* Corresponding author. Tel.: +44-7505-964184. E-mail address: mashruks@cardiff.ac.uk
https://doi.org/10.18573/jae.10

brough back the interest for the use of NH_3. Several groups are tackling the challenges concerning flame speed, emissions and practical implementation. A great variety of analysis and reviews are now available on the subject [1–5]. However, there is a new trend where efforts on the formation of species at the flame front and the use of ternary blends (ie. that include hydrogen) are gaining traction.

Nitrogen oxides in ammonia flames are mainly composed by fuel NOx (NO, NO_2 and N_2O). The conversion from the chemically bounded nitrogen to NOx emission depends on local fuel concentration and combustion characteristics. During combustion, some species such as NH_3, CN, N, HCN, and NH react to promote fuel NOx production or consumption. At low hydrogen content, it is known that the decomposition starts by the formation of OH/O/H radical pools, which interact with ammonia to form NH_i species that can lead to HNO, main molecule preceding the formation of NO [6]. N_2O, a greenhouse gas with global warming potential (GWP) 280 times than CO_2 [7], can also reach high concentration levels, as its production/consumption is dependent on the availability of NH and H radicals [8–10]. Similarly, NO_2 is a gas that can have detrimental impacts to humans. All these implications require further works that need to focus on characterizing both experimentally and numerically the reaction paths and radical interactions of these emissions for their proper abatement.

Important radicals involved in the decomposition/reaction of ammonia-hydrogen are NH_i species. Amidogen, NH_2, has been identified in ammonia reaction mechanisms since the work from Bowman in 1971 [11], whose investigations led to an improved mechanism that considered NO formation/consumption at the flame. Amidogen, formed mostly from the reaction NH_3+OH, then decomposes into imidogen, NH, preceding HNO at high temperatures (1300-1600 K) [12]. This line of work, considerably expanded over the years, has led to new insights into the impact of NH_2 and NH on ammonia flames. Amidogen has been recently analyzed by Manna et al. [13] using a Jet Stirred Flow Reactor. The work approaches the impacts of NH_2 at various temperatures, including those where the DeNOxing paths of the radical are enhanced [14]. Of great interest are the insights around the recombination of NH_2 with H_2 to reconvert amidogen back to NH_3. The reaction $NH_2+H_2 \rightarrow NH_3+H$ is assumed to be the reaction sustaining the high temperature reaction $H+O_2$. It must be noted that NH_3 does not only seems to act as an OH scavenger in NH_3-H_2 flames, but it is plausible that it acts as a third body in various reactions, acting as a strong collider to promote especially the reaction $H+O_2$ [7]. However, the role of NH_2 at higher temperatures is reduced due to its faster decomposition to NH, hence inhibiting the coupled reaction between ammonia and hydrogen. Similarly, studies conducted by Pugh et al. [15] were performed to characterize the chemiluminescence traces of NH*, NH_2* and OH* in ammonia-hydrogen flames at elevated conditions. The works denoted the importance of NH_2* as a good marker in NO consumption under rich conditions. Follow up studies [16] also raised the importance of NH_2 in the consumption of NO and the relevance of the radical in heat release, a process also correlated to OH and NH species [17, 18], all of which are sensitive to operability conditions [15, 19–21]. Other works [22–29] showed intrinsic correlations between the NH_i radicals and combustion features such as laminar and turbulent flame speeds, stretch rate, and NO profiles, whilst also denoting their impact on the production of other NOx pollutants such as N_2O [10]. Machine Learning has also been used to define equations that correlate NH_i radicals to heat release rates in ammonia-hydrogen flames [30]. Findings show correlations such as $[NH]^{0.952}[OH]^{0.062}$ and $[NH_2]^{1.039}[OH]^{0.641}$ as high reconstruction parameters for laminar flames at various equivalence ratios. Therefore, being highly relevant to the stability and emissions profile of ammonia-hydrogen blends, it is crucial that these species are understood within the context of complex turbulent flames as those employed in industrial burners.

As for the addition of other fuels to ammonia-hydrogen mixtures, the rationale lays on the transition of current power systems to fully net zero combinations. It is foreseen that the replacement of fossils using ammonia and/or hydrogen will be gradual, hence requiring at some point the use of fossils in combination with ammonia-hydrogen. This fact, combined with potential start-up scenarios that will still rely on fossil species, creates a practical case to the study of fossil-ammonia-hydrogen mixtures. Methane addition in ammonia has been extensively studied [31, 32]. However, other light alkanes such as ethane, propane or butane have received little attention although they serve a large portion of power applications. Propane was firstly analyzed when co-burning with ammonia by Cellek [33] who numerically performed a study of various flames enriched by ammonia up to 50% (vol). Ammonia-hydrogen delivered the highest NOx emissions out of the blends analyzed, whilst ammonia-propane showed similar levels to methane, although the former blend showed slightly longer flames. It was also found that an increase of ammonia would also impact emissions with a sudden NO reduction at high ammonia levels and low equivalence ratios. Laminar burning velocities were also investigated numerically and

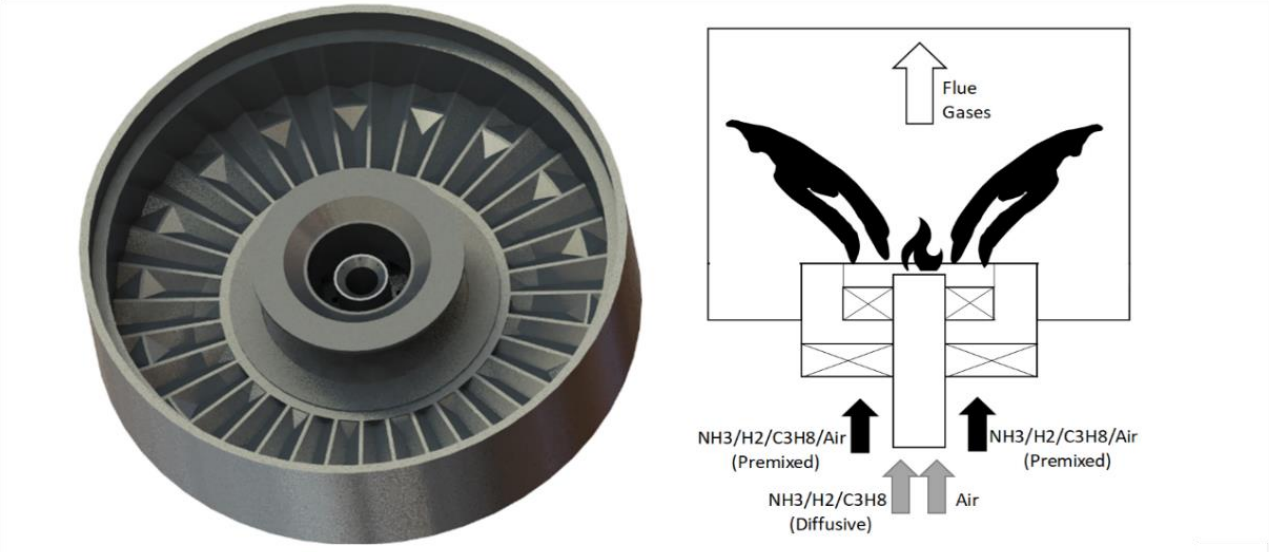

Fig. 1. Schematic of the burner

experimentally by Wang [34]. Various pressures and ammonia contents were also analyzed to observe the behavior of these flames to define Markstein lengths, flame thickness, Zeldovich and Lewis numbers. The effective Lewis number does not seem to be affected at the studied pressures (up to 0.5MPa), although it was affected by equivalence ratio, whilst flame thickness decreases and Zeldovich number increases with pressure (although thickness eventually becomes insensitive to higher pressures). Being flame thickness a parameter that characterizes hydrodynamic instabilities and Lewis number an insensitive value to pressure, it was found that when observing cellularization at the flame this was caused mainly by hydrodynamic instabilities in these flames. Markstein lengths decrease with the increase of equivalence ratio, similar to propane-air flames. Although more propane leads to more O/H radical pools, there seems to be no significant change in the mixture heating value or combustion efficiency when using different ammonia concentrations (i.e. due to the similar mixture heating values of ammonia and propane), whilst carbon emissions can be considerably reduced when replacing C_3H_8 with NH_3 [34]. NH_2 demonstrated to be an important contributor in the combustion process of ammonia-propane blends. Further analyses conducted by Wang et al. [35] also showed how ammonia's OH scavenging effect on OH and H is also a dominant parameter when using light alkane molecules. Hence, using ammonia fraction for laminar flame speed and CO_2 reduction might be the most practical engineering approach to the use of these blends.

Further, the need to reduce carbon and keep higher flame speeds would require the use of ternary blends that might include hydrogen recoverable from ammonia cracking, eventually replacing fossil molecules completely. Thus, the present work provides evidence of the effect of fuel switching using ternary blends composed by ammonia/hydrogen/propane in air. Similar work, conducted by Mashruk et al. [36] denotes how the variation in species can have a critical impact on flame features and emissions profiles when using methane. Hence, the addition of ternary flame analyses has also been included to provide further guidance in the use of these potential blends whilst using novel burners combined with non-intrusive radical analyses.

The paper is divided in various sections, namely the methods employed, followed by results obtained using stratified combustion and ternary blends in a novel gas turbine burner, respectively. Finally, conclusions are drawn to summarize the most important findings of this work.

Materials and Methods

This work employed a newly designed stratified gas turbine combustion burner, Fig. 1, at Cardiff University. The system allows both premixed and diffusive operability modes with up to 3 different fuels. A premixed tangential swirler with a geometric swirl number of $S_g = 1.05$ was employed. Fuel and air flows were supplied using dedicated Bronkhorst mass flow controllers (±0.5% within a range of 15-95% mass flow). Supplied H_2 had two entry points – one for premixing with air and ammonia, another around the central injector to burn with the aid of surrounding air. A $70/30_{vol.\%}$ NH_3/H_2 blend which has shown comparable behavior to methane flames [15, 37, 38] was chosen for the initial study at different percentages of H_2

stratification (0-100%) and three different global equivalence ratios (0.8, 1.0 and 1.2).

For the ternary blends analysis, the burner was used in premixed mode, hence reducing uncertainties with respect to the use of the central injector with these blends (a topic for future work). Ternary blends stability zones were obtained with three constant $H_{2vol.\%}$ = 10, 30 and 50%. In addition, ammonia/propane and ammonia/hydrogen stability maps were also investigated. Experiments were conducted at atmospheric pressure (1.1 bara) and inlet temperature (288 K) with a constant fuel inlet thermal power of 10 kW. All the experimental points used to determine the stable zones were repeated at least three times with error bars incorporated to visualise measurement uncertainties. A Logitech C270 camera was used to monitor the flame stability at a distance of 5 m from the combustor.

A pair of LaVision CCD cameras were employed to obtain line-of-sight chemiluminescence traces of various species. The units were triggered simultaneously at a frequency of 10 Hz with constant gain. A range of optical (Edmund) filters were used for each species of interest, namely OH* (309 nm; $A^2\Sigma^+$–$X^2\Pi$ system) [39], NH* (336 nm; $A^3\Pi$–$X^2\ \Sigma^-$ system) [39–42] and NH_2* (630 nm; single peak of the NH_2 α band) [39, 43].

Work using NO Planar Laser Induced Fluorescence (PLIF) appears as a relevant method to adequately characterise the formation of NO species [44]. Hence, 2-D NO-PLIF data was obtained by exciting NO species at 235.782 nm. A 10 Hz Nd:YAG laser (Continuum Powerlite™ Precision II) operating at the third-harmonic (355 nm) was used to pump a dye laser (Sirah Cobra-Stretch) operating on Coumarin 102 dye solution. The dye has a peak of 473 nm, which then doubled to produce an output wavelength of ~236 nm. The offline signal was recorded at 235.803 nm and subtracted from the online signal to minimise interference. Shot-to-shot variations were recorded using LaVision Davis 10 system and corrected for the acquired data.

Temperature profiles were obtained via K and R type thermocouples feeding a data logger with a frequency of 1 Hz. Thermocouple data were taken for 120 s for each point and averaged. Exhaust emissions (NO, N_2O, NO_2, NH_3, CO, CO_2, O_2 and H_2O) were measured using a bespoke Emerson CT5100 Quantum Cascade Laser analyser at a frequency of 1 Hz, a repeatability of ±1%, 0.999 linearity, and sampling temperature up to 190°C. A heated line at 160°C was employed to avoid condensation and capture exhaust samples. A dilution methodology was introduced by adding N_2 in the sample using a high precision Bronkhorst EL-FLOW Prestige Mass Flow Controller (MFC). The N_2 then heated up to 160°C by the system prior to its mixing with the exhaust samples.

Results

Effects of H_2 stratification

Figure 2 shows the changes in radicals and NO formation with increasing percentages of H_2 stratification at stoichiometry (global ϕ = 1.0). Note that the origin corresponds to the burner centreline. Measured NH_2* intensities were found to be significantly higher than OH* and NH* intensities across all flames, with NH* being the lowest among the three species. The radicals and NO formations

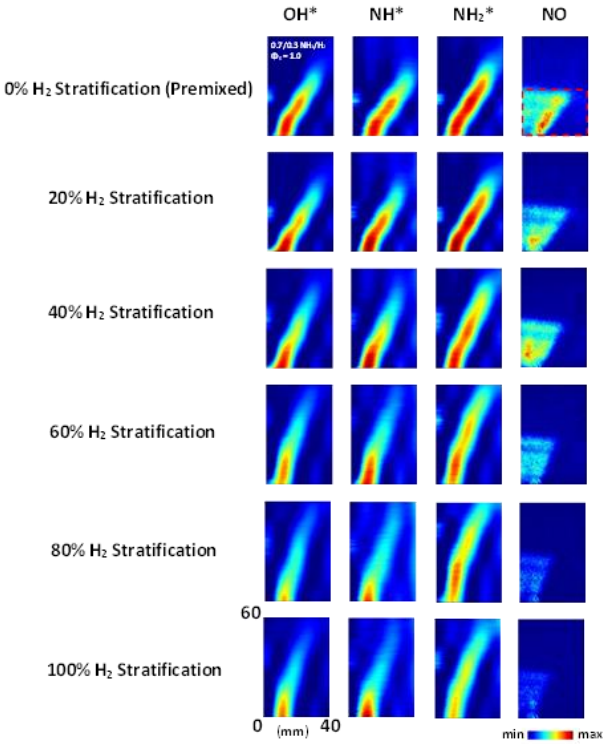

Fig. 2. Abel transformed chemiluminescence (OH*, NH* and NH_2*) and NO-PLIF images with changing H_2 stratification at stoichiometry. Colourmap for the chemiluminescence images are normalized to species dataset max. The red dashed line in the top right NO-PLIF image is the laser sheet crossing the flame.

concentrate towards the central axis as the H_2 stratification increases from the central injector. Also, OH*, NH* and NH_2* intensity decreases and concentrate closer to the burner exit with increasing H_2 stratification, which results in lower NO production in the flame zone. Earlier studies [45–47] have identified HNO as the main intermediary for NO productions with reactions NH + OH ↔ HNO + H and NH_2 + O ↔ HNO + H as the main contributors for HNO production. Similar to previous studies [15, 42, 48], a positive correlation

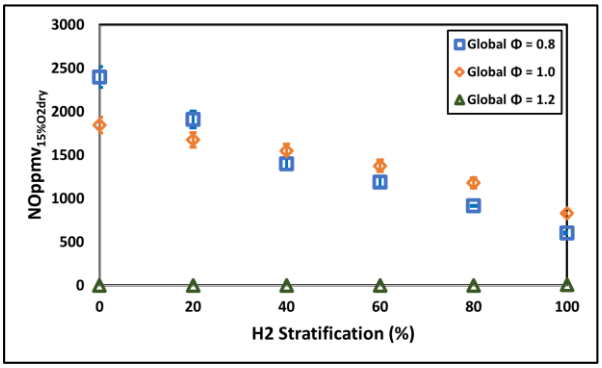

Fig. 3. Sampled NO emissions with changing H_2 stratification and ϕ.

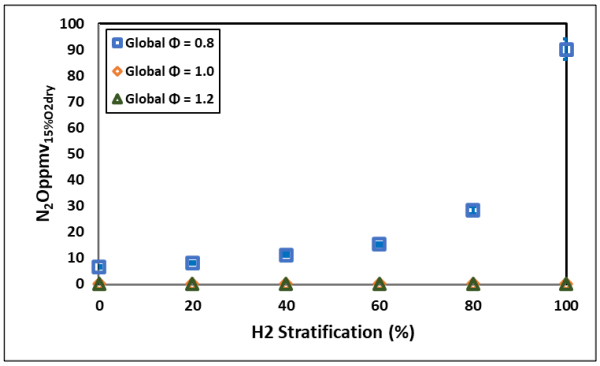

Fig. 5. Sampled N_2O emissions with changing H_2 stratification and ϕ.

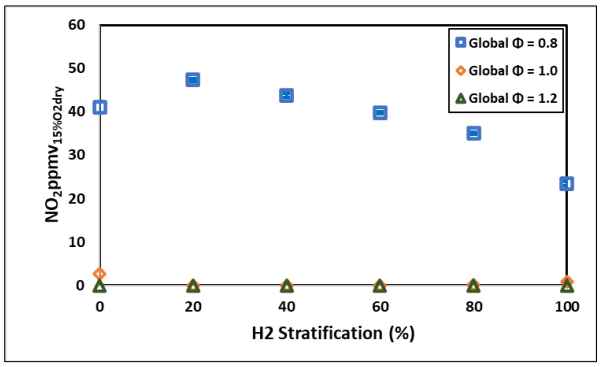

Fig. 4. Sampled NO_2 emissions with changing H_2 stratification and ϕ.

assumption between ground state and emitting species would indicate a drop in these radicals (either by reduced formation or faster consumption with other species) with increasing H_2 stratification, which will in turn reduce HNO production in combination with less O/H free radicals, thus suppressing NO formation. Temperature measured at the burner nozzle with various thermocouples also indicate drops in temperature with increasing H_2 stratification, which is in line with the measured OH* and NO intensity, as they are both temperature dependent.

Figures 3 and 4 report the measured NO and NO_2 emissions at the exhaust. Similar to NO-PLIF data, measured NO at the lean and stoichiometry conditions display decreasing trends with increasing H_2 stratification. However, NO_2 data display an increase at 20% stratification, followed by a decreasing trend. NO_2 readings were negligible at stoichiometry and rich condition, in line with previous studies conducted by Mashruk et al. [21, 37, 49]. Further kinetic analyses are necessary to understand these trends using stratified flames.

Figure 5 shows the measured N_2O emissions at the exhaust. NH_3 emissions are not reported here as

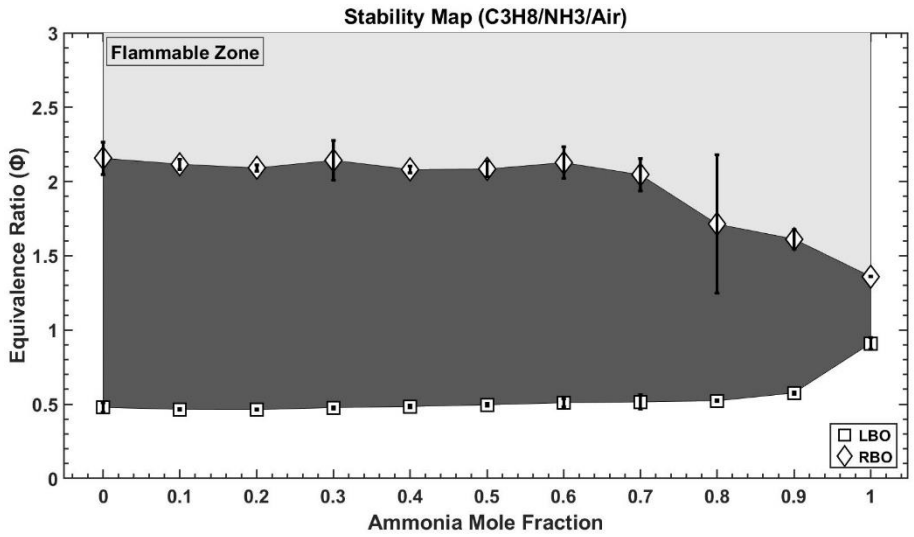

Fig. 6. Stability map of propane/ammonia flames. The dark area is the stable zone bounded by LBO and RBO.

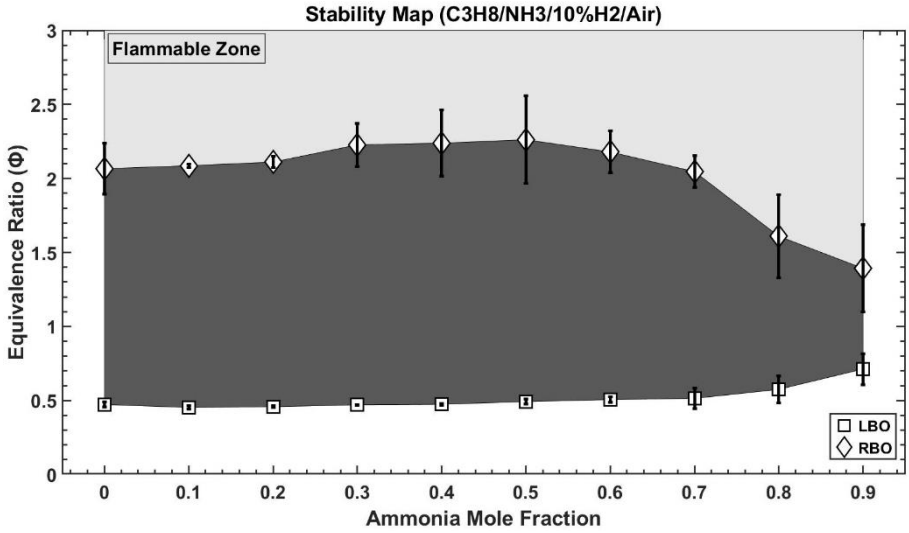

Fig. 7. Stability map of propane/ammonia/10% hydrogen flames. The dark area is the stable zone bounded by LBO and RBO.

unburnt ammonia emissions were negligible up to stoichiometry. However, concentrations were beyond the measurement capability of the analyzer passing ϕ = 1.3, suggesting the need of another equivalence ratio for improved emissions (NH_3 and NOx) and maximized performance.

Interestingly, N_2O emissions increased with increasing H_2 stratification at global Φ = 0.8, even though negligible N_2O were reported for stoichiometry and rich conditions. This could be attributed to the constant splitting ratio between fuel streams which ensures leaner premixed flames due to a decrease in H_2 flows. Previous studies [8, 9, 21] have showed the increase in N_2O formation at lean conditions ($\Phi \leq 0.7$) in ammonia-hydrogen flames due to decrease in H radical production and decreased flame temperature. Further work is required to control the air splitting ratio to avoid lean conditions at the core which enhances nitrous oxide production.

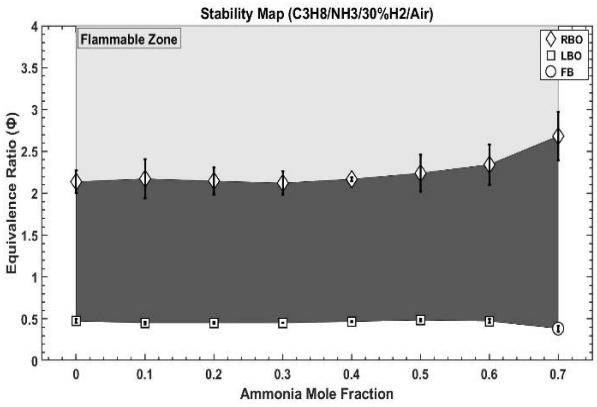

Fig. 8. Stability map of propane/ammonia/30% hydrogen flames. The dark area is the stable zone bounded by FB, LBO and RBO.

Stability Mapping

Initial operability maps using propane/ammonia binary fuels, Fig. 6, showed a decrease in stability with ammonia addition. The stable region remains somewhat constant up to $70_{vol.\%}$ NH_3 but further increase in ammonia flow reduces the stable zone severely as ammonia chemistry becomes dominant. The stable zone in propane/ammonia binary fuels are bounded by lean blow-out (LBO) and rich blow-out (RBO) zones but flashback (FB) was not observed in these binary blends as the flame speeds were not high enough to force flashback.

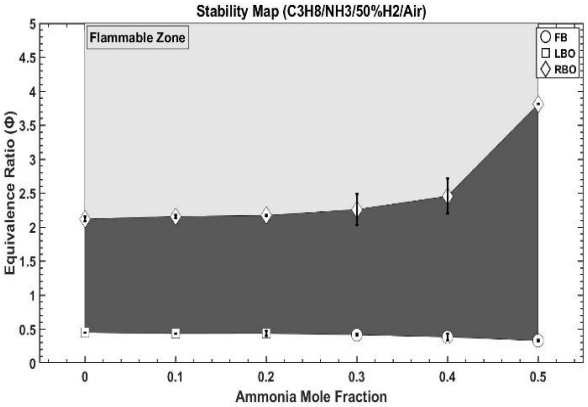

Fig. 9. Stability map of propane/ammonia/50% hydrogen flames. The dark area is the stable zone bounded by FB, LBO and RBO.

Figure 7 shows the stability map of propane/ammonia/10% hydrogen blends. Up to $20_{vol.\%}$ ammonia, the stable zone limits were similar to the binary propane/ammonia blends. However, from 30-$50_{vol.\%}$ ammonia, propane mole fraction decreases by a certain margin to allow hydrogen chemistry becoming dominant and thus enhancing the stable zone region. As ammonia mole fraction

increases beyond 50%, ammonia chemistry takes over and the stability zone shrinks.

Figures 8 and 9 show the ternary operability limits with constant $30_{vol.\%}$ and $50_{vol.\%}$ H_2, respectively. With $X_{H2} \geq 0.3$, the flashback phenomenon is observed as the flame speed increases substantially. For the $30_{vol.\%}$ hydrogen flames, the stability zone only widens when the propane mole fraction drops below 30% and performs better than $10_{vol.\%}$ H_2 scenarios. Even though flashback was only observed for the $70/30_{vol.\%}$ NH_3/H_2 blend in Fig. 3, flashback was observed for $50_{vol.\%}$ H_2 in a wider set of cases ($X_{NH3} \geq 0.3$). For these cases, $X_{NH3} \geq 0.3$, wider blow off limits were also observed due to high hydrogen and low propane presence in the blends.

Table 1. Selected blends for further analysis

Blends	C_3H_8 (vol.%)	NH_3 (vol.%)	H_2 (vol.%)
1	90	10	0
2	80	15	5
3	70	20	10
4	60	25	15
5	50	30	20
6	40	35	25
7	30	40	30
8	20	45	35
9	10	50	40
10	0	55	45
11	0	60	40
12	0	70	30

Based on the results and analysis of the operability limits, 12 blends were chosen for further analysis, Table 1. Experiments were carried out at four equivalence ratios (0.6,0.8,1.0 and 1.2) for these blends. Chemiluminescence (OH*, NH*, C_2*, NH_2*), spectrometry (200 – 1050 nm range), temperature (5 locations [8]) and exhaust emissions measurements (NO, NO_2, N_2O, NH_3, CO, CO_2, O_2 and H_2O) were taken at each point to identify possible suitable blends for decarbonization purposes. These analyses will be discussed in the following section.

Chemiluminescence Analysis

Figure 10 shows the changes in radical formation at stoichiometry for the selected blends shown in Table 1. Colourmaps are normalized to species maximum intensities to display the change of radical formation. At stoichiometry, intensities of OH*, C_2* and NH* decrease with increasing ammonia contents in the flames, whereas NH_2* follows the opposite trend. The flame thickness also increases with increasing ammonia content, a characteristic of ammonia flames discussed elsewhere [8, 36].

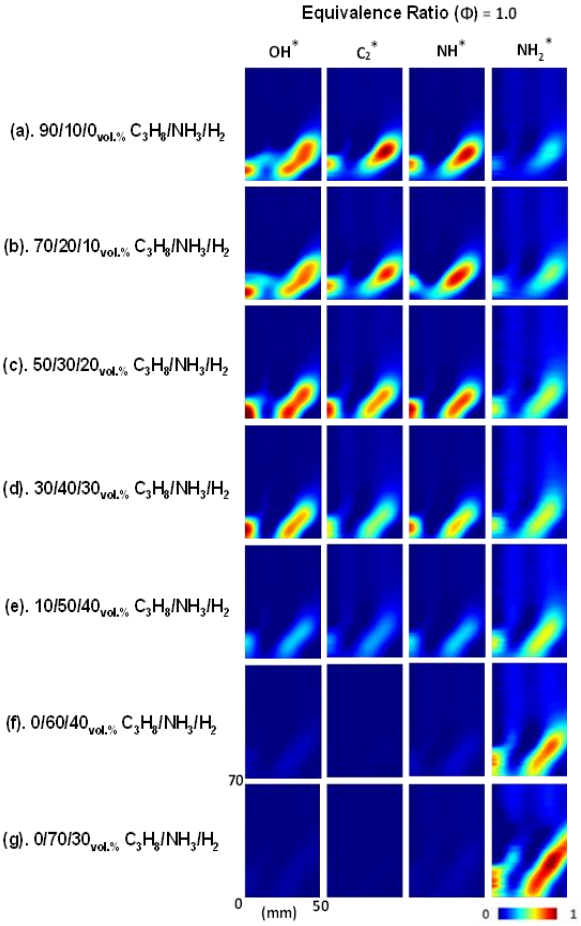

Fig. 10. Changes in radical formation at stoichiometry for the selected blends (Table 1).

Further analyses of OH* and NH_2* formations across difference equivalence ratio showed that OH* intensity peaks at $\Phi = 0.8$, while NH_2* intensity peaks at $\Phi = 1.2$. Also, OH* intensities were found to be peaking at $X_{NH3} = 0.45$ which can be attributed to the increase in H_2 content in the blend with sufficient amount of propane still present. These changes in radical formations control the emissions performances of these blends which will be analyzed next.

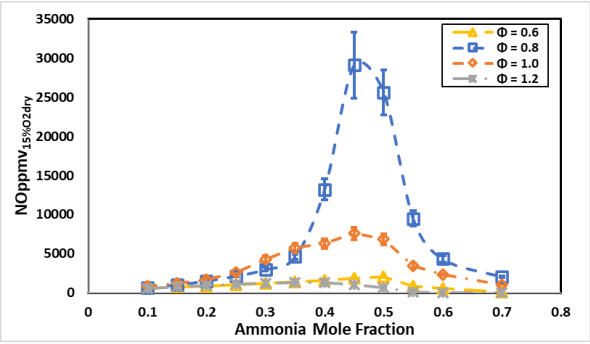

Fig. 11. Sampled NO emissions with changing blends and Φ.

Emissions Analysis

All the emissions data reported in this section are normalised to 15% O_2, dry [50]. Figures 11 and 12 show the sampled NO and NO_2 emissions across different fuel blends and changing equivalence ratios, respectively.

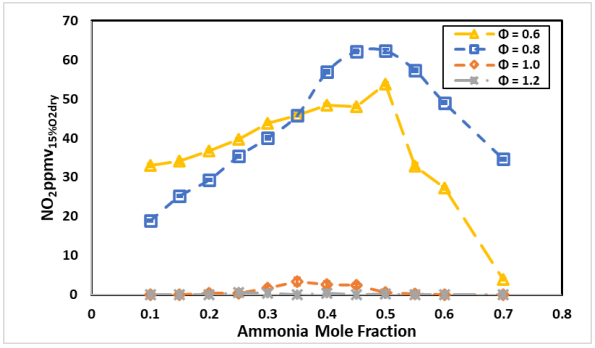

Fig. 12. Sampled NO_2 emissions with changing blends and Φ.

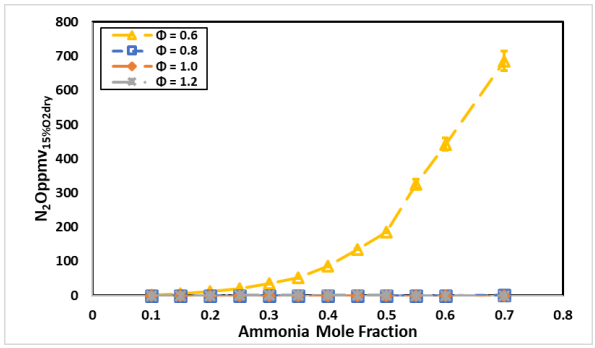

Fig. 13. Sampled N_2O emissions with changing blends and Φ.

Both NO and NO_2 peak at $\Phi = 0.8$ and $X_{NH3} = 0.45$, which coincided with maximum OH* production. This observation is in line with the findings from previous studies [36, 51]. OH reacts with NH to produce HNO through the reaction OH + NH ↔ HNO + H, which then reacts with OH, O and H radicals to produce NO. NO_2 is directly related to NO through the reactions NO + HO_2 ↔ NO_2 + OH and NO + O + M ↔ NO_2 + M and reverts back to NO by reacting with H radical [21].

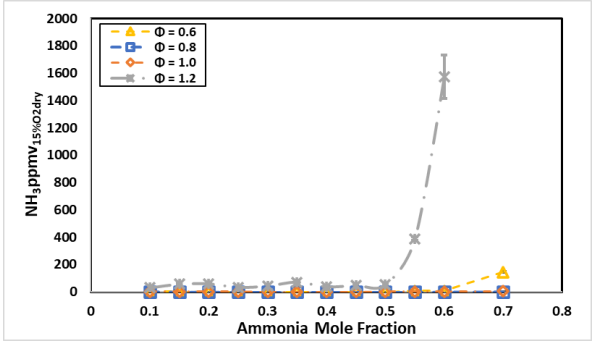

Fig. 14. Sampled NH_3 emissions with changing blends and Φ.

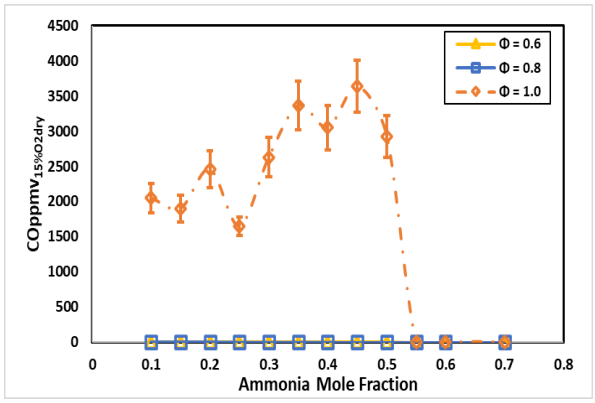

Fig. 15. Sampled CO emissions with changing blends and Φ. Rich condition not included as it was out of range.

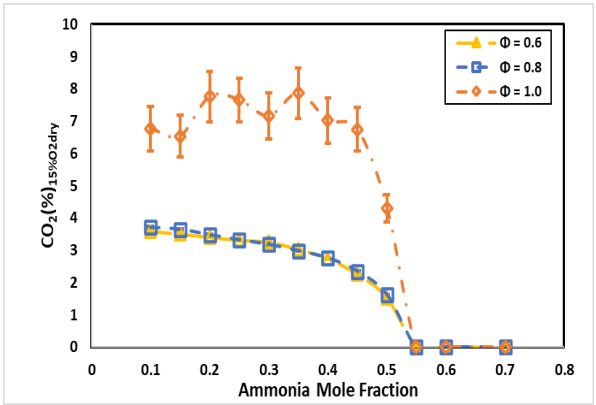

Fig. 16. Sampled CO_2 emissions with changing blends and Φ.

Sampled N_2O and NH_3 emissions for different blends with changing Φ are shown in Figs. 13 and 14, respectively. NH reacts with NO to produce N_2O in the flame but most of these N_2O reduce to N_2 through the reactions $N_2O + H \leftrightarrow N_2 + OH$ and $N_2O + M \leftrightarrow N_2 + O + M$. N_2O emissions are a concern at $\Phi = 0.6$, a phenomenon likely promoted by low H radical production and low flame temperature as shown by recent studies [8, 9, 21, 49, 52]. Unburnt ammonia emissions are also a concern for highly rich conditions, which can be averted by tunning the system to the right equivalence ratio and through implementation of staged combustion [45, 53, 54]. At $\Phi = 1.2$, unburnt ammonia emissions increase significantly at $X_{NH3} > 0.5$. Below $50_{VOL.\%}$ ammonia content in the fuel, high presence of propane ensures significant OH production which reduces ammonia through the reaction $NH_3 + OH \leftrightarrow NH_2 + H_2O$.

Negligible CO emissions were found at the lean conditions considered here but a high amount of CO

was observed at the stoichiometry and rich conditions, Fig. 15. This was caused by the incomplete combustion of propane. CO_2 emissions decreases with increasing ammonia content in the fuel, Fig. 16. CO_2 emissions at the lean conditions followed each other very closely.

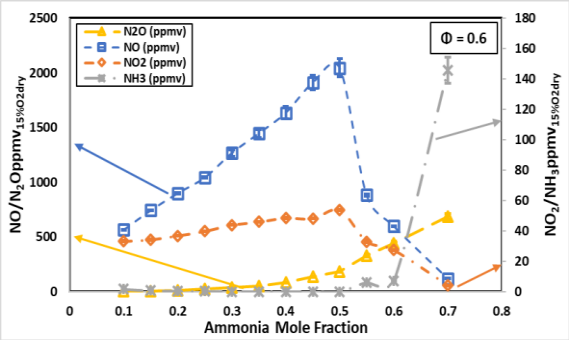

Fig. 17. Sampled NO, NO_2, N_2O and NH_3 emissions with changing blends at $\Phi = 0.6$.

From the above analysis, $\Phi = 0.6$ cannot be considered for retrofitting in current industrial combustion systems, Fig. 17, unless Selective Catalytic Reduction (SCR) is available on-site. NOx emissions were found to be quite high for all the blends at $\Phi = 0.6$. No carbon monoxide emissions were observed for these blends and CO_2 emissions were below 4%, Fig. 16. These ternary blends can be considered for existing combustion systems with SCR systems in place during the transition stage towards zero carbon fuels. Further, emissions above $30_{VOL.\%}$ ammonia blends at $\Phi = 0.6$ considerable worsen when employing the studied combustion set-up, with NO and NO_2 emissions increasing significantly and thus limiting the use of these blends.

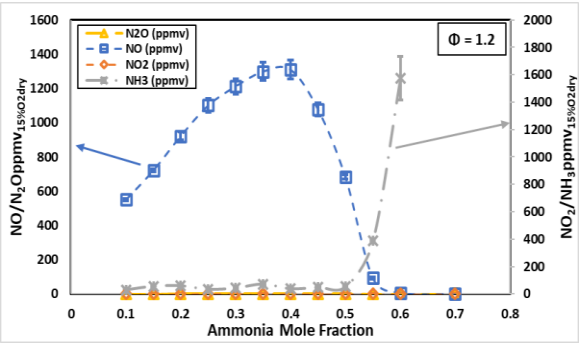

Fig. 18. Sampled NO, NO_2, N_2O and NH_3 emissions with changing blends at $\Phi = 1.2$.

However, the use of stratification, as in the previous section, could be the solution to these blends. At $\Phi = 1.2$, the mixtures show high CO and CO_2 (out of range), although NO emissions significantly dropped with low propane content, Fig. 18. Interestingly, NO emissions peaked at $X_{NH3} = 0.5$ and 0.4 for $\Phi = 0.6$ and 1.2, respectively. This can be attributed to high flame temperatures due to increased hydrogen content in the fuel mixtures which results into higher NO production through HCN route (HCN → CN → NCO → NO) [12]. Also, higher OH under lean conditions. However, further increase in ammonia contents in the fuel mixtures enhances NH_2 production, thus reducing NO production. Further kinetic work is recommended to understand this phenomenon. NH_3 emissions suddenly increased passing $X_{NH3} > 0.55$. However, there seems to be an ideal spot at which both NOx and unburned ammonia are at their minimum. This "sweet" location could be improved using hydrogen stratification, as in the previous section or employing staged combustion technologies which can finish the combustion of any remaining CO, whilst also making good use of any remaining hydrogen in the flue gases. Such a technology promises to drop significantly unburned fuel traces with NOx emissions [55–57]. Furthermore, transition towards pure ammonia/hydrogen blends will ensure absolute zero carbon emissions.

Conclusions

A new burner was used to evaluate the impacts of stratification using ammonia-hydrogen flames, whilst also supporting the analysis of ternary blends that include propane.

Effects of hydrogen stratification in premixed ammonia/hydrogen/air flames were investigated for the first time in a novel burner. The data shows a decrease in OH*, NH* and NH_2* radicals productions with increase in H_2 stratification, which in turn reduces NO and NO_2 formation. However, N_2O emissions increases at global lean condition as hydrogen availability is reduced in the mixing zone. Further work is necessary to avoid these induced lean zones by changing air splitting ratios.

Stability maps of fully premixed $C_3H_8/NH_3/H_2$ ternary blends in such a burner were also defined. Increase of hydrogen mole fractions widened the operability limits, as expected, given that other two fuel mole fractions were in a certain range to allow hydrogen to take over the flame chemistry. For $X_{NH3} \geq 0.7$ and $X_{H2} \leq 0.2$, ammonia chemistry becomes dominant and shrinks the operability regions. Based on these results, 12 blends were chosen for further detailed analyses. NO and NO_2 emissions peaked at $\Phi = 0.8$ and $X_{NH3} = 0.45$ due to the high presence of OH/O/H radicals. Significant amount of N_2O emissions were observed at $\Phi = 0.6$ for $X_{NH3} > 0.3$

due to lower production of H radicals and low flame temperatures. High unburnt ammonia emissions were observed for ammonia-hydrogen blends due to a lower production of OH radicals. Significant amounts of CO emissions were observed at $\Phi \geq 1.0$ due to incomplete combustion of propane. The analyses highlight the difficulties with retrofitting the existing systems at low equivalence ratio conditions with these ternary blends. Meanwhile, the $\Phi = 1.2$ case shows great promise with ammonia mole fraction at 0.55. Although CO will be highly produced, the pollutant can be fully converted into CO_2 by using staged burner systems without any SCR system, hence supporting the reduction of CO_x and NO_x emissions with low ammonia traces, emissions that could be reduced further with stratification techniques.

Acknowledgments

This work was supported by the AMBURN project with funding from the Department for Business, Energy & Industrial Strategy (BEIS). The research was undertaken at Cardiff University's Thermofluids Lab (W/0.17) with invaluable technical support from Mr. Malcolm Seaborne. Information on the data underpinning the results presented here, including how to access them, can be found in the Cardiff University data catalogue at http://doi.org/10.17035/d.2023.0257310177.

Conflicts of Interest

The authors declare no conflict of interest. The funders had no role in the design of the study; in the collection, analyses, or interpretation of data; in the writing of the manuscript, or in the decision to publish the results.

References

1. Kobayashi H., Hayakawa A., Somarathne K. D. K. A., and Okafor E. C. Science and technology of ammonia combustion', *Proc Combust Inst.* 2019 37(1): 109–133, doi: https://doi.org/10.1016/j.proci.2018.09.029.

2. Valera-Medina A. et al. Review on Ammonia as a Potential Fuel: From Synthesis to Economics, *Energy Fuels.* 2021;35(9): 6964–7029, doi: https://doi.org/10.1021/acs.energyfuels.0c03685.

3. Elbaz A. M., Wang S., Guiberti T. F., and Roberts W. L. Review on the recent advances on ammonia combustion from the fundamentals to the applications, *Fuel Comms.* 2022;10: 100053, doi: https://doi.org/10.1016/j.jfueco.2022.100053.

4. Kang L., Pan W., Zhang J., Wang W., and Tang C. A review on ammonia blends combustion for industrial applications, *Fuel.* 2023; 332: 126150, doi: 10.1016/j.fuel.2022.126150.

5. Boero A. J. et al., Environmental life cycle assessment of ammonia-based electricity, *Energies (Basel).* 2021; 14(20):6721, doi: https://doi.org/10.3390/EN14206721/S1.

6. Tomidokoro T., Yokomori T., and Im H. G. Numerical study on propagation and NO reduction behavior of laminar stratified ammonia/air flames, *Combust Flame.* 2022; 24, doi: https://doi.org/10.1016/j.combustflame.2022.112102.

7. Greenhouse Gas Protocol, 'Global Warming Potential Values', 2007. [Online]. Available: https://www.ghgprotocol.org/sites/default/files/ghgp/ Global-Warming-Potential-Values%20%28Feb%2016%202016%29_1.pdf (Accessed: Jul. 30, 2021).

8. Mashruk S. et al. Evolution of N2O production at lean combustion condition in NH3/H2/air premixed swirling flames, *Combust Flame.* 2022; 244: 112299. doi: https://doi.org/10.1016/j.combusflame.2022.112299.

9. Hayakawa A., Hayashi M., Gotama G., Kovaleva M., Okafor E., and Colson S., Mashruk S., Valera-Medina A. and Kobayashi H. N2O production characteristics of strain stabilized premixed laminar ammonia/hydrogen/air premixed flames in lean conditions, in 13th Asia-Pacific Conf Combust, 2021.

10. Hayakawa A. et al. Experimental and numerical study of product gas and N2O emission characteristics of ammonia/hydrogen/air premixed laminar flames stabilized in a stagnation flow, *Proc Combust Inst.* 2022, doi: https://doi.org/10.1016/j.proci.2022.08.124.

11. Bowman C. T. Investigation of Nitric Oxide Formation Kinetics in Combustion Processes: The Hydrogen-Oxygen-Nitrogen Reaction, *Combust Sci Tech.* 2007; 3(1): 37–45, doi: https://doi.org/10.1080/00102207108952269.

12. Glarborg P., Miller J. A., Ruscic B., and Klippenstein S. J. Modeling nitrogen chemistry in combustion, *Prog Energy Combust Sci*, vol. 67, pp. 31–68, Jul. 2018, doi: 10.1016/j.pecs.2018.01.002.

13. Manna M. V., Sabia P., Sorrentino G., Viola T., Ragucci R., and de Joannon M. New insight into NH3-H2 mutual inhibiting effects and dynamic regimes at low-intermediate temperatures, *Combust Flame.* 2022: 111957, doi: https://doi.org/10.1016/j.combustflame.2021.111957.

14. Klippenstein S. J., Harding L. B., Glarborg P., and Miller J. A. The role of NNH in NO formation and control, *Combust Flame* . 2011;158(4): 774–789, doi: https://doi.org/10.1016/j.combustflame.2010.12.013.

15. D. Pugh et al. An investigation of ammonia primary flame combustor concepts for emissions reduction with OH*, NH2* and NH*

chemiluminescence at elevated conditions, *Proc Combust Inst*. 2021; 38(4):6451–6459, doi: https://doi.org/10.1016/j.proci.2020.06.310.

16. Mashruk S. et al. Numerical Analysis on the Evolution of NH2 in Ammonia/hydrogen Swirling Flames and Detailed Sensitivity Analysis under Elevated Conditions, *Combust Sci Tech*. 2021;195(6): 1251-1278, doi: https://doi.org/10.1080/00102202.2021.1990897.

17. Brackmann C., Nilsson E. J. K., Nauclér J. D., Aldén M., and Konnov A. A. Formation of NO and NH in NH3-doped CH4 + N2 + O2 flame: Experiments and modelling, *Combust Flame*. 2018; 194:278–284, doi: https://doi.org/10.1016/j.combustflame.2018.05.008.

18. Li J., Huang H., Deng L., He Z., Osaka Y., and Kobayashi N. Effect of hydrogen addition on combustion and heat release characteristics of ammonia flame, *Energy*, vol. 175, pp. 604–617, May 2019, doi: https://doi.org/10.1016/j.energy.2019.03.075.

19. Khamedov R. A Computational Study of Ammonia Combustion, King Abdullah University of Science & Technology, Thuwal, 2020. [Online]. https://repository.kaust.edu.sa/handle/10754/663983 (Accessed Dec. 30, 2022).

20. Jin T., Dong W., Qiu B., Xu C., Liu Y., and Chu H. Effect of Ammonia on Laminar Combustion Characteristics of Methane-Air Flames at Elevated Pressures, *ACS Omega*, 2021, doi: https://doi.org/10.1021/acsomega1C05938.

21. Mashruk S. et al. Nitrogen oxide emissions analyses in ammonia/hydrogen/air premixed swirling flames, *Energy*. 2022; 260:125183, doi: https://doi.org/10.1016/j.energy.2022.125183.

22. Zhu X., Khateeb A. A., Roberts W. L., and Guiberti T. F. Chemiluminescence signature of premixed ammonia-methane-air flames, *Combust Flame*. 2021; 231:111508, doi: https://doi.org/10.1016/j.combustflame.2021.111508.

23. Wang S., Elbaz A. M., Arab O. Z., and Roberts W. L. Turbulent flame speed measurement of NH3/H2/air and CH4/air flames and a numerical case study of NO emission in a constant volume combustion chamber (C.V.C.C.), *Fuel*. 2023;332: 126152, doi: https://doi.org/10.1016/j.fuel.2022.126152.

24. Zitouni S., Brequigny P., and Mounaim-Rousselle C. Turbulent flame speed and morphology of pure ammonia flames and blends with methane or hydrogen, *Proc Combust Inst*. 2022, doi: https://doi.org/10.1016/j.proci.2022.07.179.

25. Thomas D. E., Shrestha K. P., Mauss F., and Northrop W. F. Extinction and NO formation of ammonia-hydrogen and air non-premixed counterflow flames, *Proc Combust Inst*. 2022, doi: https://doi.org/10.1016/j.proci.2022.08.067.

26. Mashruk S., Zhu X., Roberts W. L., Guiberti T. F., and Valera-Medina A. Chemiluminescent footprint of premixed ammonia-methane-air swirling flames, *Proc Combust Inst*. 2022, doi: https://doi.org/10.1016/j.proci.2022.08.073.

27. Vigueras-Zúñiga M. O., Tejeda-Del-Cueto M. E., Mashruk S., Kovaleva M., Ordóñez-Romero C. L., and Valera-Medina A. Methane/Ammonia Radical Formation during High Temperature Reactions in Swirl Burners, *Energies*. 2021; 14(20):6624, doi: https://doi.org/10.3390/EN14206624.

28. Zhu X., Khateeb A. A., Guiberti T. F., and Roberts W. L. NO and OH* emission characteristics of very-lean to stoichiometric ammonia-hydrogen-air swirl flames, *Proc Combust Inst*. 2021: 5155–5162. doi: https://doi.org/10.1016/j.proci.2020.06.275.

29. Zhu X., Roberts W. L., and Guiberti T. F. UV-visible chemiluminescence signature of laminar ammonia-hydrogen-air flames, *Proc Combust Ins*. 2022, doi: https://doi.org/10.1016/j.proci.2022.07.021.

30. Chi C., Sreekumar S., and Thévenin D. Data-driven discovery of heat release rate markers for premixed NH3/H2/air flames using physics-informed machine learning, *Fuel*. 2022; 330:125508, doi: https://doi.org/10.1016/j.fuel.2022.125508.

31. Valera-Medina A., Mashruk S., Pugh D., and Bowen P. Ammonia, *Renewable Fuels*. 2022:245–274, doi: https://doi.org/10.1017/9781009072366.011.

32. Valera-Medina A. and Banares-Alcantara R., Techno-Economic Challenges of Green Ammonia as an Energy Vector, 1st ed. Academic Press, 2021. doi: https://doi.org/10.1016/c2019-0-01417-3.

33. Cellek M. S. The decreasing effect of ammonia enrichment on the combustion emission of hydrogen, methane, and propane fuels, *Int J Hydrogen Energy*. 2022; 47(45):19916–19934, doi: https://doi.org/10.1016/j.ijhydene.2021.11.241.

34. Wang Z., Ji C., Wang D., Zhang T., Zhai Y., and Wang S. Experimental and numerical study on laminar burning velocity and premixed combustion characteristics of NH3/C3H8/air mixtures, *Fuel*. 2023;331:125936, doi: https://doi.org/10.1016/j.fuel.2022.125936.

35. Wang D. et al. A comparative study on the laminar C1–C4 n-alkane/NH3 premixed flame, *Fuel*. 2022; 324:124732, doi: https://doi.org/10.1016/j.fuel.2022.124732.

36. Mashruk S. et al. Combustion features of CH4/NH3/H2 ternary blends, *Int J Hydrogen Energy*. 2022;260: 125183, doi: https://doi.org/10.1016/j.ijhydene.2022.03.254.

37. Mashruk S., Zitouni S.-E., Brequigny P., Mounaim-Rousselle C., and Valera-Medina A.

Combustion performances of premixed ammonia/hydrogen/air laminar and swirling flames for a wide range of equivalence ratios, *Int J Hydrogen Energy*. 2022; 47(97) 41170–41182, doi: https://doi.org/10.1016/j.ijhydene.2022.09.165.

38. Verkamp F. J., Hardin M. C., and Williams J. R., Ammonia combustion properties and performance in gas-turbine burners, in *Symp (Int) Combust.* 1967: 985–992. doi: https://doi.org/10.1016/S0082-0784(67)80225-X.

39. Gaydon A., The spectroscopy of flames. 2012. [Online]. Available: https://link.springer.com/book/10.1007/978-94-009-5720-6 (Accessed Sep. 17, 2021)

40. Ohashi K., Kasai T., Che D. C., and Kuwata K. Alignment dependence of the amidogen chemiluminescence in the reaction of argon(3P) atoms with the aligned ammonia molecules, *J Phys Chem*. 2002; 93(14):5484–5487, doi: https://doi.org/10.1021/J100351A033.

41. Schott G. L., Blair L. S., and Morgan J. D. Exploratory shock-wave study of thermal nitrogen trifluoride decomposition and reactions of nitrogen trifluoride and dinitrogen tetrafluoride with hydrogen, *J Phys Chem.* 2022; 77(24): 2823–2830, 2002, doi: https://doi.org/10.1021/J100642A001.

42. Roose T. R., Hanson R. K., and Kruger C. H. A shock tube study of the decomposition of no in the presence of NH3, *Symp (Intl) Combust*. 1981;18(1): 853–862, doi: https://doi.org/10.1016/S0082-0784(81)80089-6.

43. Yi Y., Zhang R., Wang L., Yan J., Zhang J., and Guo H. Plasma-Triggered CH4/NH3 Coupling Reaction for Direct Synthesis of Liquid Nitrogen-Containing Organic Chemicals, *ACS Omega*. 2017;2(12): 9199–9210, doi: https://doi.org/10.1021/acsomega.7b01060.

44. Wang G., Tang H., Yang C., Magnotti G., Roberts W. L, and Guiberti T. F. Quantitative laser-induced fluorescence of NO in ammonia-hydrogen-nitrogen turbulent jet flames at elevated pressure, *Proc Combust Inst.* 2022, doi: https://doi.org/10.1016/j.proci.2022.08.097.

45. Mashruk S., Xiao H., and Valera-Medina A. Rich-Quench-Lean model comparison for the clean use of humidified ammonia/hydrogen combustion systems, *Int J Hydrogen Energy*. 2020; 46(5): 4472–4484, doi: https://doi.org/10.1016/j.ijhydene.2020.10.204.

46. Zhang M. et al. The regulation effect of methane and hydrogen on the emission characteristics of ammonia/air combustion in a model combustor, *Int J Hydrogen Energy*. 2021; 46(40):21013–21025, doi: https://doi.org/10.1016/j.ijhydene.2021.03.210.

47. Xiao H., Lai S., Valera-Medina A., Li J., Liu J., and Fu H. Study on counterflow premixed flames using high concentration ammonia mixed with methane, *Fuel*. 2020; 275:117902, doi: https://doi.org/10.1016/j.fuel.2020.117902.

48. Sheehe S. L. and Jackson S. I. Spatial distribution of spectrally emitting species in a nitromethane–air diffusion flame and comparison with kinetic models, *Combust Flame*. 2020; 213: 184–193, doi: https://doi.org/.1016/j.combustflame.2019.10.026.

49. Mashruk S., Kovaleva M., Chong C. T., Hayakawa A., Okafor E., and Valera-Medina A. Nitrogen Oxides as a By-product of Ammonia/Hydrogen Combustion Regimes, *Chem Eng Trans*. 2021; 89: 613–618, doi: https://doi.org/10.3303/CET2189103.

50. British Standard, 'BS 1SO 11042-1:1996. Gas Turbines-Exhaust Gas Emission', 1996.

51. An Z. et al. Emission prediction and analysis on CH4/NH3/air swirl flames with LES-FGM method, *Fuel*. 2021; 304: 121370, doi: https://doi.org/10.1016/j.fuel.2021.121370.

52. Alnasif A., Mashruk S., Kovaleva M., Wang P., and Valera-Medina A. Experimental and Numerical Analyses of Nitrogen Oxides formation in a High Ammonia-Low Hydrogen Blend using a Tangential Swirl Burner, *Carbon Neutrality*. 2022; 1(24), doi: https://doi.org/10.1007/s43979-022-00021-9.

53. Guteša Božo M., Mashruk S., Zitouni S., and Valera-Medina A. Humidified ammonia/hydrogen RQL combustion in a trigeneration gas turbine cycle, *Energy Convers Manag*. 2021; 227: 113625, doi: https://doi.org/10.1016/j.enconman.2020.113625.

54. Somarathne K. D. K. A., Okafor E. C., Sugawara D., Hayakawa A., and Kobayashi H. Effects of OH concentration and temperature on NO emission characteristics of turbulent non-premixed CH4/NH3/air flames in a two-stage gas turbine like combustor at high pressure, *Proc Combust Inst*. 2021; 38(4):5163–5170, doi: https://doi.org/10.1016/j.proci.2020.06.276.

55. Okafor E. C. et al. Towards the development of an efficient low-NOx ammonia combustor for a micro gas turbine, *Proc Combust Inst*. 2019; 37(4): 4597–4606, doi: https://doi.org/10.1016/j.proci.2018.07.083.

56. Iki N. et al. Nox reduction in a swirl combustor firing ammonia for a micro gas turbine, *Proc ASME Turbo Expo*. 2018. doi: https://doi.org/10.1115/GT201875993.

57. Somarathne K. D. K. A. et al. Emission characteristics of turbulent non-premixed ammonia/air and methane/air swirl flames through a rich-lean combustor under various wall thermal boundary conditions at high pressure, *Combust Flame*. 2019; 210: 247–261, doi: https://doi.org/10.1016/j.combustflame.2019.08.037.